

The authors thank the reviewers for their very constructive comments. Aside from minor changes and typo corrections, all changes and comment responses are included below. Reviewer comments are shown in **bold** and the author responses are indented. Changes to the manuscript are shown in ~~red~~ and blue text.

RC1: ‘Comment on egusphere-2024-552’, Anonymous Referee # 1, 17 May 2024

This paper relates theoretically turbulent features and cloud geometry features (mainly perimeter). Then, estimates of the latter on numerous satellite data as well output of numerical simulation enable to confirm previously developed framework to address the issue of anisotropy of turbulence across scales. In general, I found the paper well written and conclusions relevant for the community. I believe that only minor modifications are needed, mainly to improve clarity and help the reader through the numerous equations/approximations and data sets.

General comments:

- Calling “Xi” (Greek letter) the spatial resolution is a bit confusing, because it often called “scale” with resolution being the ratio between outer scale and observation scales. On a similar point, it is not clear to me why either “l” or “xi” are used whereas it seems to me that they both represent the observation scale at which the studied geometrical set/field is studied. Could you please clarify.

The choice of ξ as the variable for spatial resolution follows its use in [1] which relates cloud perimeters to ξ and to the turbulent eddy diffusion. Rather than normalizing by the outer scale L , instead ξ is normalized by η following e.g., [2, 1] to relate the cloud perimeter to turbulent eddy diffusivity.

ξ was chosen to link in a straightforward manner cloud perimeters measured by satellites with a range of native spatial resolutions (ξ_N) to the fractal dimension through Eqns. (1) and (8), following the “ruler length” definition of D and D_e [4, 3]. ξ is also related to the box-counting dimension where each box is represented by a pixel in a satellite image.

Revised l. 23-24:

(defined as either the pixel side length in a satellite image or the grid spacing in a model following Garrett et al. (2018)).

Added the following to l. 149-151:

Note that ξ is normalized here by η rather than its common normalization by an outer scale L (Lovejoy, 2023). We choose this normalization to more conveniently relate \mathcal{P}_ξ to K_ξ and K_η .

- A summary with the main formulas that are first theoretically derived and then validated with data would be helpful for the reader. May be in the form of a figure or table.

Added the following table summarizing the main formulas:

Table 1: Summary of main formulas

Equation number	Formula	Reference
(1)	$p \propto \xi^{1-D}$	Mandelbrot (1967)
(2)	$S(\ell) = \Delta\Theta(\ell) = \langle \Theta(x + \ell) - \Theta(x) \rangle \propto \ell^{\mathcal{H}}$	Kolmogorov (1941)
(3)	$K \sim \ell^{1+\mathcal{H}}$	Derived from Richardson (1926) and Kolmogorov (1941)
(4)	$D = 2 - \mathcal{H}$	Hentschel and Procaccia (1984)
(5)	$K\mathcal{P} = \mathcal{N}\xi_V$	Garrett et al. (2018)
(6)	$\mathcal{P}_\xi \sim \frac{\mathcal{N}\xi}{K_\xi}$	Equation (5)
(7)	$K_\xi = K_\eta \left(\frac{\xi}{\eta}\right)^{1+\mathcal{H}}$	Krueger et al. (1997) and Eq. (3)
(8)	$\mathcal{P}_\xi = \frac{\mathcal{N}\eta}{K_\eta} \left(\frac{\eta}{\xi}\right)^{\mathcal{H}} \propto \xi^{-\mathcal{H}}$	Equations (6) and (7)
(9)	$\mathcal{P}_\xi \propto \xi^{1-D_e}$	Mandelbrot (1977)
(10)	$K_\xi \propto \xi^{D_e}$	Equations (6) and (9)
(11)	$\mathcal{H} = D_e - 1$	Equations (8) and (9)
(12)	$D_e = 3 - D$	Equations (4) and (11)

- It would be interesting to discuss results of Fig. 4 in light of the scaling relation between perimeter and area which is reminded l. 38.

Revised l. 309-311:

The ensemble fractal dimension that corresponds to the total cloud perimeter given by Eq. (11) is $D_e = \mathcal{H} + 1 = 1.78 \pm 0.09$, larger than the canonical value $D \approx 4/3$ often observed for individual clouds obtained using the expression $p \propto \sqrt{a}^D$.

- For some of the analysed fields, you have 3D data. Why not trying an analysis in 3D directly instead of reconstructing a 2D field before carrying out the analysis ?

The next paragraph clarifies that we perform the analysis on generated 2D cloud fields from SAM to represent how the cloud ensembles are viewed by satellite, including any overlap. Added clarification to the lines where SAM is introduced.

Revised l. 231-234:

As a means to compare measurements of \mathcal{P}_ξ from satellite observations to the value derived by Garrett et al. (2018), we ~~include measurements of clouds from~~ consider the geometries of clouds simulated using the System for Atmospheric Modeling (SAM), calculated as they would be viewed from space. SAM is a high-resolution 3D LES, initialized with idealized GATE Phase III campaign soundings for tropical convection.

- It should be clarified better how a pixel is set to cloudy or not during the coarsening process. Indeed, many of the observed process depends on this. See detailed comments below.

Added to Figure 3 (shown below) a diagram to describe the coarsening process with clarifying text added to the caption.

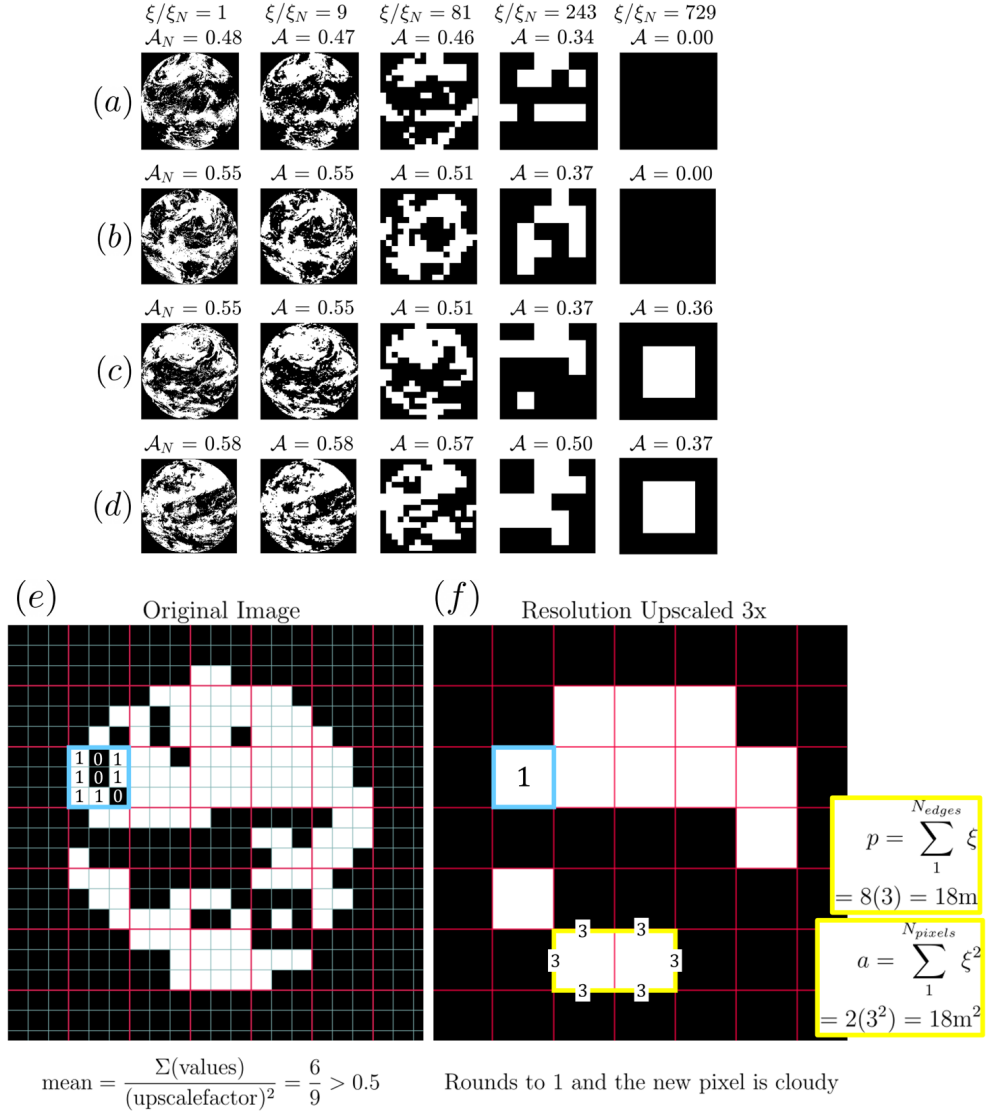


Figure 3: Top: EPIC cloud masks shown at native resolution ξ_N and coarsened resolutions ξ to a single pixel for four cases with initial native cloud fraction between $0.48 < \mathcal{A}_N < 0.58$ (increasing from top to bottom) illustrating a bifurcation of cloud fraction with coarsening of resolution depending on the native cloud fraction to either zero or unity. Note that the single pixel case shown here has a value of $\mathcal{A} = 0.37$ rather than unity because the domain area represented by the square pixel is the disk area $A_d = \pi a^2$. Bottom: A detailed example of the upscaling method. The “original” image here is shown at 100x the resolution of the true original image to exaggerate pixels for clarity, and the coarsened image is upscaled 3x or $k = \xi/\xi_N = 3$. The thin blue lines outline pixels with side lengths ξ_N and the red boxes are the upscaled pixel regions. An example region of pixels from which the mean is used to determine whether the upscaled pixel is cloudy or clear is highlighted as a thick blue box with pixel values shown within. An example of the individual perimeter and area calculation is highlighted in yellow, assuming the original pixel resolution is $\xi_N = 1$ m. Areas outside the circle are marked NaN and so are omitted from the average.

Revised l. 247-255:

To obtain values of D_e , total cloud perimeter P is calculated first at the native spatial resolution ξ_N and normalized by A_d to obtain \mathcal{P}_N . The image is then artificially coarsened (see description below) and the procedure is repeated. \mathcal{P}_ξ is obtained at progressively coarser spatial resolutions $\xi > \xi_N$ such that $\xi = \xi_N k$, where k is the coarsening factor. ~~The image is coarsened by reducing the number of pixel elements by k^2 . Coarsening is performed by separating the original image into a grid of multiple “boxes” containing $k \times k$ pixels (see Fig. 3e, red boxes) which are reduced to a single upscaled pixel through averaging. Each pixel of the coarsened image (Fig. 3f, outlined in blue) is determined to be cloudy or clear by rounding the average of the values from the corresponding pixels inside each box in the native resolution image (Fig. 3e, outlined in blue) to unity or zero.~~

Detailed comments:

- l. 54-55: please clarify what you mean.

Revised l. 55-61:

~~This multifractal~~ The multifractal nature of clouds and their apparent size and type dependence of D seems seem to contradict the arguments of Lovejoy (1982) that cloud fractal properties are consistent across scales. However argument that cloud geometries are scale invariant. Additionally, a monofractal, scale-invariant assumption might more reasonably describe a D does not account for multifractal parameters that account for turbulent intermittency (the variability of turbulent fluctuations), notably observed in measurements of water mixing ratio (Tuck, 2022). However, scale-invariance might be a reasonable assumption for describing a large ensemble of clouds considered over a sufficiently long period of time and space, especially if turbulent intermittency might be reflected by the geometric intermittency of multiple and varied cloud types in the ensemble. Indeed, the topic of whether or how scale invariance can describe applies to atmospheric structures has been the topic of decades of debate (Lovejoy and Schertzer, 2018).

- Eq. 2: it assumes no intermittency correction.

Revised l. 68-69:

Along one dimension x , the generalized first-order (which ignores intermittency) “structure function” expresses the covariance of Θ as a function of separation distance ℓ .

- Eq. 8: please provide more explanations on how is obtained.

Revised l. 58-61:

From a climatological perspective, it is instead the ensemble of clouds with total perimeter density \mathcal{P} that governs exchanges of energy and air across cloud edges. ~~Accordingly, we introduce~~ Following the fractal “islands” analogy from Mandelbrot (1977) who considered the total perimeter of an ensemble of objects (described in more detail below), we propose an “ensemble fractal dimension” for clouds D_e analogous to Eq. (1) such that ...

- l. 171: please explain better the notation D_μ and how it is used.

Added to l. 111-112:

Equation (4) has also been related directly to cloud perimeter fractal dimension as adjusted for intermittency μ through $D_\mu = 2 - \mathcal{H}$ (Hentschel and Procaccia (1984)).

Revised l. 188-190:

Applying the canonical value of $D = 4/3$ for individual clouds leads to the expected value of $D_e = 5/3$ ~~—for cloud ensembles.~~ Perhaps the geometric intermittency of multiple and varied cloud types in an ensemble reflects the turbulent intermittency that is not represented by D for individual clouds. This is in agreement with Hentschel and Procaccia (1984), who found that Richardson’s 4/3 law only applies if the fractal dimension is $D_\mu = 5/3$, obtained by adding an intermittency correction with a value between $0.25 < \mu < 0.5$ to the value $D = 4/3$.

- l. 177: the issue of the intermittency correction is briefly mentioned here. There could also be one in eq. 2. I believe that this issue and its implications on the various equations used should be clarified.

The change made to l. 188-190 in the previous comment also addresses this comment. Additionally, see the revision to l. 68-69:

Along one dimension x , the generalized first-order (which ignores intermittency) “structure function” expresses the covariance of Θ as a function of separation distance ℓ .

- l. 187-190: a scheme on how \mathbf{P} and \mathbf{A} are computed in practice would be helpful, and also how observation scale is changed.

Added more detail about how p and a are computed and included a brief example in the revised Figure 3.

Revised l. 203-208:

The quantities p and a are calculated for all individual ~~cloudy regions, which clouds~~ (see Fig. 3f for an example). The perimeter is defined as the sum of all pixel edge lengths along the outer edge of each cloud. Although the example shows that all pixel sizes are equal, in satellite imagery, each pixel has individual values of ξ_x and ξ_y for its width and height, which are adjusted from ξ_N to account for the Earth’s curvature away from the satellite nadir vertically and horizontally. The area is the sum of $\xi_x \times \xi_y$ for each pixel in the cloud. For each image, p and a are summed and normalized by domain area A_d to determine \mathcal{P} and \mathcal{A} .

- l. 232-233: what is done once the rounding is implemented ? This approach and its impact should be discussed with regards to a common approach when computing fractal dimension that would be a consider a coarser pixel as cloudy it at least one of the pixels is contains at higher resolution is cloudy.

This point is clarified in the revised Figure 3.

- Fig. 3: how are side effect due the round shape handled ?

The round shape becomes increasingly square during coarsening, and the rounding method simply omits NaN values for pixels beyond the disk. The method of excluding NaNs is sufficient up to coarsening factors $k = \xi/\xi_N \sim 100$. The boxy examples are included to demonstrate the extreme case of coarsening.

Added the clarifying text to the caption of Figure 3:

Areas outside the circle are marked NaN and so are omitted from the average.

- In general for section 3: a table with a summary of the data used would be helpful for the reader.

Added the following table summarizing the satellite datasets used:

Table 2: Summary of satellite datasets used in this study.

Dataset name	Sensor name	View Type	Approx. nadir resolution	Longitude at nadir	Dates examined	Description of cloud mask algo
MODIS 250 m	MODIS	Polar-Orbiting	250 m	-	01 January 2021 to 09 January 2021	DeWitt et al. (2019)
VIIRS	VIIRS	Polar-Orbiting	750 m	-	03 June 2021 to 04 June 2021	Kopp et al. (2021)
MODIS 1km	MODIS	Polar-Orbiting	1 km	-	02 June 2012 to 02 June 2012	Ackerman et al. (2012)
Himawari	AHI	Full-Disk	2 km	141° E	02 June 2021 to 01 July 2021	Derrien and Glèzet (2021)
GOES	ABI	Full-Disk	2 km	137° W	02 June 2021 to 01 July 2021	Derrien and Glèzet (2021)
METEOSAT	SEVIRI	Full-Disk	3 km	0°	02 June 2021 to 01 July 2021	Derrien and Glèzet (2021)
EPIC	EPIC	Full-Disk	8 km	-	01 January 2017 to 31 January 2017	Yang et al. (2019)
GeoRing	(Composite)	Full-Disk	11 km	-	02 June 2021 to 21 June 2021	Ceamanos et al. (2021)

- Section 4.1: it is not clear to me why this bifurcation is observed ? How sensitive is it to how a pixel is set to cloudy or not at coarser resolution, which is not very clear for me now ?

The revision to Figure 3 provides more clarification about how a pixel is set to cloudy or clear during coarsening.

Revised l. 271-275:

This bifurcation of cloud fraction reflects that as an image of a cloud field is coarsened to a single pixel, ~~that pixel will either have a value of the coarsened pixel value is determined by averaging and rounding to zero or unity, depending on whether the pixel values in the original image (illustrated in Sect. 3). Conversely, a coarsening method in which the presence of any cloudy pixel in the original image results in a cloudy coarsened pixel causes cloud fraction to converge to unity with coarsening (Di Grlamo and Davies, 1997). Due to this averaging method, the value to which cloud fraction bifurcates depends on the native cloud fraction is greater or less than $A_N = 0.55A_N$.~~

- Section 4.2 and Fig. 4.b: Can the range of scales used to perform linear be clarified ? Native scale is excluded but seems inserted in straight lines visible in Fig. 4.b. Points for high values of ξ/ξ_N also seem to deviate from the straight line. Indicators of the quality of the linear regression should be added and discussed. Again how sensitive are results to the way a coarser pixel is set to cloudy or not ?

Added clarification about the linear regression methods and data points used for the fit.

Revised l. 256-259:

A least squares linear regression is performed on values of $\ln \mathcal{P}_\xi$ and $\ln \xi$ to obtain the Hurst exponent \mathcal{H} and D_e from Eqs. (8) and (9). Linear regression was performed on the straightest region of all curves, which was found to be $7 < \xi/\xi_N < 150$ where biases due to interpolation ($\xi/\xi_N < 7$, most significantly for EPIC) and due to the square shape of pixels at very coarse resolutions ($\xi/\xi_N > 150$) are omitted. Uncertainties in the linear regression are evaluated at the 95% confidence level.

Added to the caption of Figure 4:

Linear regression was performed on the straightest portion of all curves, found to be $7 < \xi/\xi_N < 150$, although the best fit lines are extrapolated to all points to show their relative distance to the fit.

Added to l. 291-293:

For $\xi > \xi_N$, \mathcal{P}_ξ is well characterized by a linear regression of $\ln \mathcal{P}_\xi$ to $\ln \xi$ (Eq. 8). Linear regression is performed only on data points in the straightest region of all curves, $7 < \xi/\xi_N < 150$, where biases due to interpolation ($\xi/\xi_N < 7$) and the square shape of pixels at very coarse resolutions ($\xi/\xi_N > 150$) are ignored. The lines in the figure are shown extrapolated to all points to demonstrate their relative distance to the least-squares fit, which can be assumed to more reliably reflect the physical fractal nature of the cloud ensemble.

Citation: <https://doi.org/10.5194/egusphere-2024-552-RC1>

RC2: ‘Comment on egusphere-2024-552’, Anonymous Referee #2, 27 May 2024

GENERAL

This is a thorough study of the scaling characteristics of clouds as observed by satellites, both orbiters and geostationaries. The basic result is important confirmation of the relevance statistical multifractal studies of atmospheric variables. It is well worthy of publication.

COMMENTARY

Comments are located by line number.

14: The atmosphere is not materially closed. Water has large fluxes in and out, with a residence time of about 10 days. Fluxes of gases such as carbon dioxide, methane, nitrous oxide, halocarbons and ozone also occur, with lifetimes spanning days to centuries. Even the major constituents oxygen (10^4 years) and nitrogen (10^6 years) are not “materially closed”. In addition, volcanology has intermittent effects, and aerosols are injected by various processes, including wave breaking and industrial activity.

Revised l. 15:

The ~~atmosphere~~-Earth system is radiatively open and materially closed.

Revised l. 17-18:

Materially, the total dry atmospheric mass is confined to the planet by gravity and can only be redistributed by turbulent circulations that mix air ~~and moisture~~ over a broad range of scales within the thin atmospheric layer.

15: Inspection of outgoing longwave radiation observed by satellites doesn’t look isotropic to this reviewer.

Revised l. 15-17:

Radiatively, Earth’s global mean temperature is sustained by a balance between absorption of high-intensity shortwave sunlight ~~that is reemitted nearly isotropically and~~ the reemission at longwave frequencies to the cold of space.

54-56: Restricting characterization to D omits the roles of intermittency C1 and Lévy exponent α . That matters especially for water, the material of clouds. See the departures from 5/9 in Figure 13 of <https://doi.org/10.3390/meteorology1010003>

Revised l. 55-61:

~~This multifractal~~-The multifractal nature of clouds and their apparent size and type dependence of D ~~seems seem~~ to contradict the ~~arguments of Lovejoy (1982) that cloud fractal properties are consistent across scales. However~~argument that cloud geometries are scale invariant. Additionally, a monofractal ~~-, scale-invariant assumption might more reasonably describe a~~ D ~~does not account for multifractal parameters that account for turbulent intermittency (the variability of turbulent fluctuations), notably observed in measurements of water mixing ratio (Tuck, 2022). However, scale invariance might be a reasonable assumption for describing a~~ large ensemble of clouds considered over a sufficiently long period of time and space, especially if turbulent intermittency might be reflected by the geometric intermittency of multiple and varied cloud types in the

ensemble. Indeed, the topic of whether or how scale invariance ~~can describe~~ applies to atmospheric structures has been the topic of decades of debate (Lovejoy and Schertzer, 2018).

69: Schertzer and Lovejoy, On the dimension of atmospheric motions, Turbulence and Chaotic Phenomena in Fluids, pp.505-508, T. Tatsumi ed., Elsevier North Holland, (1984) deserve at least equal credit with Henschel and Procaccia and arguably precedence with a 1983 preprint.

Included the reference in l. 73.

Caption, Figure 1. The results of Alder & Wainwright (1970), Phys. Rev.1, 18-21 suggest that isotropic molecular diffusion is never relevant in the atmosphere. See <https://doi.org/10.3390/meteorology1010003>

Added the following to l. 96-98:

Furthermore, the results of Alder and Wainwright (1970) show the formation of vortices even at the 10^{-8} m scale, inconsistent with a description of isotropic molecular diffusion (Tuck, 2022).

165: Large eddy simulation imposes a cubic symmetry on the air that it does not have. What it has is continuous translational symmetry.

Added the following to l. 179-180:

For comparison with a LES model of a tropical cloud field resolved at 100 m scales, Garrett et al. (2018) applied a value of $\mathcal{H} = 1/3$ to Eq. (7) consistent with Richardson (1926) and the 4/3 law. Implicit in this case is an assumption of 3D isotropic turbulence at resolved scales. The assumption may be appropriate for an LES that chooses a cubic Eulerian grid for computational ease at the expense of losing a Lagrangian perspective.

248: The polar orbiters are moving at ~ 7 km/s, unlike the geostationaries.

The authors are reluctant to speculate that this is a possible explanation for the differences since EPIC is also nearly geostationary and has results similar to the polar orbiters.

261: Models assume local thermodynamic equilibrium, which has been argued not to apply. See Figure 3 of Meteorology 2023, 2(4), 445- 463; <https://doi.org/10.3390/meteorology2040026>

Added to l. 285-287:

A possible explanation for the discrepancy is that models assume local thermodynamic equilibrium, which has been argued not to apply in the atmosphere (Tuck, 2022).

284-286: See comment about line 261.

Revised l. 315-317:

Note that modeled values of \mathcal{H} lie closer to the value of 1/3 expected for 3D isotropic turbulence than ~~is the case for the inferred from the~~ satellite datasets, perhaps reflecting the smaller domain area and atmospheric regime or ~~the subgrid-scale turbulence assumption-assumptions~~ used in LES models of subgrid-scale turbulence or local thermodynamic equilibrium.

Citation: <https://doi.org/10.5194/egusphere-2024-552-RC2>

References

- [1] Timothy J Garrett, Ian B Glenn, and Steven K Krueger. “Thermodynamic constraints on the size distributions of tropical clouds”. In: *Journal of Geophysical Research: Atmospheres* 123.16 (2018), pp. 8832–8849.
- [2] Steven K. Krueger, Chwen-Wei Su, and Patrick A. McMurtry. “Modeling Entrainment and Finescale Mixing in Cumulus Clouds”. In: *Journal of the Atmospheric Sciences* 54.23 (1997), pp. 2697–2712.
- [3] Benoit Mandelbrot. *Fractals*. Freeman San Francisco, 1977.
- [4] Benoit Mandelbrot. “How long is the coast of Britain? Statistical self-similarity and fractional dimension”. In: *Science* 156.3775 (1967), pp. 636–638.